ORIGINAL PAPER

Characterization of optical, thermal and electrical properties of SWCNTs/PMMA nanocomposite films

**Jalila Al-Osaimi · Najm Al-Hosiny ·
Said Abdallah · Ali Badawi**

Abstract The optical, thermal and electrical behavior of single-wall carbon nanotubes (SWCNTs)/poly(methyl methacrylate) (PMMA) composite are studied as a function of SWCNTs concentration. The nanocomposites were prepared in the form of films by solution casting technique. The concentrations of SWCNTs in SWCNTs/PMMA films were 0, 0.5, 1, 1.5, 2, 3.5, 5, 7.5, and 10 wt%. High-resolution transmission electron microscopy showed that SWCNTs doped in PMMA is less fragmented as compared to the powder SWCNTs. This is due to the interactions with polymers as well as the fabrication method. X-ray diffraction patterns of SWCNTs/PMMA composite films indicated that there is no covalent interaction between SWCNTs and PMMA. In addition, it demonstrates a homogeneous dispersion of SWCNTs in PMMA matrix. The optical properties of SWCNTs/PMMA films of SWCNTs concentration from 0 to 2.0 wt% have shown that the absorption intensity of the composite was enhanced ≈ 8.5 times as compared to the plain PMMA. Photoacoustic spectroscopy technique was used as a powerful and non-destructive tool to determine the thermal diffusivity (α), thermal effusivity (e) and thermal conductivity (k). The composites exhibited $\approx 160\%$ improvement in k at 2.0 wt%. Furthermore, the DC electrical conductivity measurements of SWCNTs/PMMA showed that the percolation threshold value was about 2.0 wt% of SWCNTs loading.

Keywords SWCNTs/PMMA composite · Photoacoustic · Optical properties · Thermal properties · DC electrical properties

J. Al-Osaimi · N. Al-Hosiny · S. Abdallah · A. Badawi (✉)
Department of Physics, Faculty of Science, Taif University,
Taif 21974, Saudi Arabia
e-mail: adaraghmeh@yahoo.com

N. Al-Hosiny
Department of Physics, Faculty of Science, Aljouf University,
Aljouf, Saudi Arabia

S. Abdallah
Department of Mathematical and Physical Engineering, Faculty
of Engineering (Shoubra), Benha University, Cairo, Egypt

Introduction

In the last two decades, carbon nanotubes (CNTs) have attracted significant scientific attention because of their superior properties, such as low weight, very high aspect ratio, high thermal conductivity, electrical conductivity, and elastic moduli [1–3]. These outstanding properties of CNTs make them an attractive candidate for making novel composites of CNTs in a series of host polymer matrices with multifunctional features [4, 5]. Therefore, CNTs/polymer nanocomposites are a new class of promising materials for potential applications, such as photovoltaic cells, transport layers and light emitting diodes (LEDs) [6]. However, the efficient utilization of CNTs for fabricating nanocomposites depends on homogeneous dispersion of CNTs within the polymer matrices [7, 8].

Photoacoustic (PA) technique is a photothermal detection technique; that is, proved to be a powerful tool to study the optical, electronic and thermal properties of such materials without particular sample treatment in a non-destructive manner [9]. PA method has gained more popularity due to its simple, elegant experimental technique as well as the versatility in employing different configurations to measure the required thermophysical parameters with great accuracy [10]. Moreover, there have been some

efforts to exploit the electrical conductivity of CNTs to develop new materials as conductive polymers or anti-static coatings [11].

In this work, we have employed PA technique to investigate the SWCNTs concentration dependence of thermophysical properties [thermal diffusivity (α), thermal effusivity (e) and thermal conductivity (k)]. Different levels of single-walled carbon nanotubes (SWCNTs) were added to poly(methyl methacrylate) (PMMA) to form composite films using casting solution technique. The optical absorption measurements of SWCNTs/PMMA composite films were performed for different concentrations of CNTs from 0 to 2.0 wt%. Furthermore, the DC electrical conductivity of the prepared films was also studied.

Experimental

Preparation of SWCNTs/PMMA nanocomposite films

The composite films of SWCNTs/PMMA with different SWCNTs concentrations were prepared using solution casting method as follows: PMMA solution was prepared by dissolving PMMA (Sigma Aldrich) in chloroform (Fluka) with weight ratio of 1:27. The solution was stirred for long time (24 h). Nanocomposite films of SWCNTs/PMMA were prepared by adding the desired weight of SWCNTs powder (Chengdu Organic Chemicals Co., China) to the above solution and stirred for 4 h on a magnetic stirrer. The produced mixture was cast in Petri dishes and left in a ventilated fuming hood till it completely dried and solidified. Nine films were obtained of PMMA + x wt% SWCNT, where $x = 0, 0.5, 1, 1.5, 2, 3.5, 5, 7.5$, and 10 wt% of thicknesses 58, 49, 48, 53, 57, 60, 58, 62, and 60 μm, respectively. The dried films were reasonably homogeneous and clear.

Measurements

The optical properties measurements were carried out using a Jasco double-beam UV–vis spectrophotometer (model V-670) within wavelength range of 200–3,000 nm. In addition, the dimension of SWCNTs was measured by a Jeol high-resolution transmission electron microscope (JEM-2100 operated at 200 kV and equipped with Gatan CCD higher resolution camera).

X-ray diffraction patterns were carried out with an automated powder diffractometer (Bruker D8-advace diffractometer) with Cu X-ray tube (wavelength: $k_{\alpha 1} = 1.540598$), the tube potential was 40 kV and the tube current was 40 mA.

PA measurements were carried out by gas microphone detection method. The light beam from 200 mW (514 nm) argon ion laser (Melles Griot, Carlsbad, CA 92009) was mechanically modulated by optical mechanical chopper (SR540), and focused on to the sample which was carefully mounted inside a PA cell (MTEC Model 300). The sound wave generated from the sample was subsequently detected as an acoustic signal by a high-sensitive electrical microphone fixed in the PA cell. The PA signal was then amplified by a low-noise preamplifier and further processed using a lock-in amplifier (Stanford Research System, Model SR830 DSP). A personal computer was interfaced to the system for automatic data acquisition and analysis. A schematic diagram of the PA experimental set-up for thermal properties measurements was shown in our previous work [12]. All the measurements were carried out at room temperature.

The DC electrical conductivity (σ) of SWCNTs/PMMA composite films was measured using a standard two-point contact method (sandwich like) on rectangular film slabs in an Oxford Optistat cryostat at room temperature. An electrometer type Keithly 6517B and an Oxford temperature controller IT053 were connected to a personal computer (PC) via GPIB interface TNT5004 card and the data was recorded by a PC.

Results and discussion

High-resolution transmission electron microscopy (HRTEM)

Figure 1 shows the TEM image of SWCNTs/PMMA at concentration of 2.0 wt%, while the inset shows a high-resolution TEM image of SWCNTs. The estimated outer

Fig. 1 TEM image of SWCNTs/PMMA composite film at concentration of 2.0 wt%, the inset shows higher resolution TEM image of SWCNTs
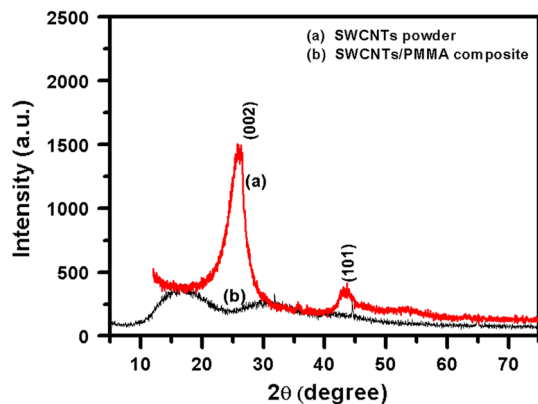
Fig. 2 X-ray diffraction patterns of: **a** SWCNTs in powder form and **b** SWCNTs/PMMA composite films at SWCNTs concentration of 0.5 wt%

Fig. 3 Optical absorption spectra of SWCNTs/PMMA nanocomposites with SWCNTs concentrations: **a** 0, **b** 0.5 wt%, **c** 1.0 wt%, **d** 1.5 wt%, and **e** 2.0 wt%

diameter is <2 nm and length of 5–30 μm. It is clearly observed that CNTs doped in PMMA is less fragmented compared to the powder case. This is due to the interactions with polymers as well as the fabrication method.

Structural properties (X-ray diffraction measurement)

Figure 2a, b show X-ray diffraction patterns of SWCNTs in a powder form and SWCNTs/PMMA composite films at a concentration of 0.5 wt%, respectively. From Fig. 2a, it is easily seen that there are three dominant peaks at $2\theta = 26.6°$, 43.45° and 54.7°, which correspond to the hexagonal graphite structures (002), (101) and (004) phases, respectively. Although Fig. 2b shows the broad bands diffraction peaks at $2\theta = 17°$ and 32° corresponding to PMMA [13], which indicates its amorphous nature. This behavior indicates that there is no covalent interactions between SWCNTs and PMMA [14]. In addition, this may prove a homogeneous dispersion of SWCNTs in PMMA matrix. Similar results have been obtained by Oh et al. [15]. In their work, they concluded the absence of CNTs peaks in X-ray diffraction pattern in CNT/TiO$_2$ composite for photo-degradation activity.

Optical absorption measurements

The absorption spectra of SWCNTs/PMMA nanocomposite films for various concentrations in the wavelength range of 1,000–2,100 nm are shown in Fig. 3. Absorption spectra of the composite films show a drastic increase in the intensity with respect to that of PMMA for SWCNTs concentrations. It is clearly seen that as the SWCNTs concentration increases, the absorption increases at the same time, due to the significant incorporation for low concentrations of SWCNTs in composite films. This
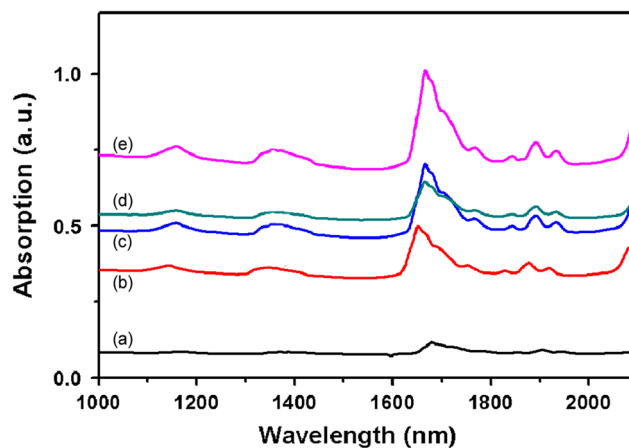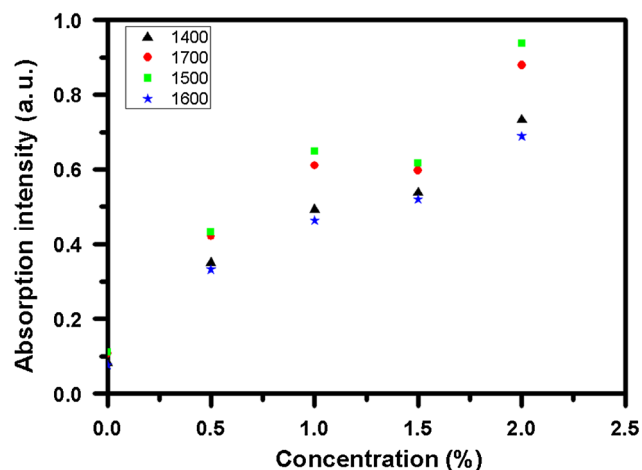

Fig. 4 Absorption intensity of SWCNTs/PMMA vs. SWCNTs concentration at different wavelengths

indicates that in the blend, an electronic interaction takes place between the two materials. The absorption intensity increases nearly 8.5 times when SWCNTs concentrations increase to 2.0 wt% as compared to the plain PMMA. In addition, we observed that the highest peak absorption was at 1,670 nm. This peak originally belongs to the polymer as can be seen in the pure spectrum (denoted in Fig. 3a).

For further clarification of the dependence of intensity on SWCNTs concentrations in the films, we draw directly this relation for different wavelengths as shown in Fig. 4. We can see that the intensity is enhanced almost linearly as the concentration is increased. Although the relation is believed to be linear, there is slight damp in the intensity at 1.5 wt% concentration. This might be due to slight inhomogeneous distribution in that sample or slight change in the sample thickness.

Fig. 5 ln(PA signal amplitude) vs. ln(*f*) of SWCNTs/PMMA nanocomposites with SWCNT concentrations: **a** 0.5 wt% and **b** 2.0 wt%
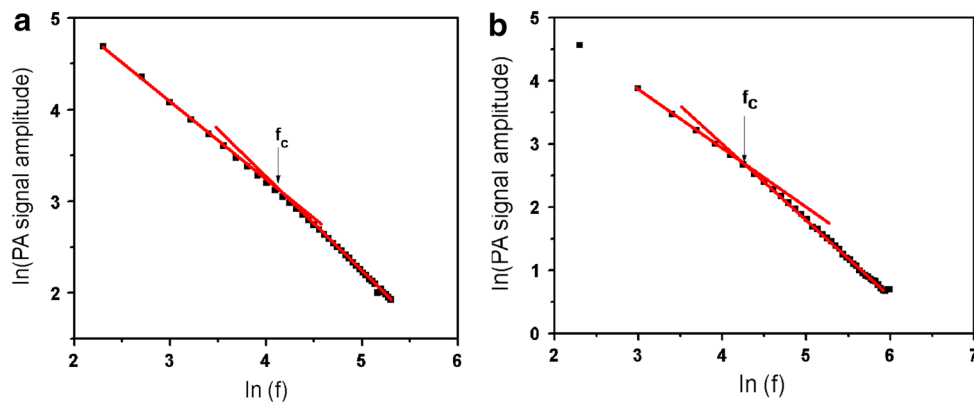
Thermal properties measurements

The thermal diffusivity (α) is an important physical quantity to be determined for a material since it is an intrinsic property in the bulk regime. This quantity gives an indication to the rate at which the heat is distributed in a material [16] and this rate depends not only on the thermal conductivity (k), but also on the rate at which the energy can be stored [17–19]:

$$\alpha = \frac{k}{\rho c} \text{ in m}^2/\text{s} \tag{1}$$

where ρ is the density and c is the specific heat capacity of the sample.

α is calculated from the characteristic frequency (f_c), which is the modulation frequency at which the sample goes from thermally thick region to the thermally thin region [17, 20]. The PA signal varies with ω^{-1} in case of optically opaque and thermally thin samples ($\mu_\beta < L$, $\mu_S > L$, $\mu_S > \mu_\beta$) [10, 21], while in case of thermally thick samples, the thermal diffusion length, μ_s, is smaller than the optical absorption length, μ_β, the PA signal varies with $\omega^{-3/2}$ [10]. So, at f_c, there is a distinct change in the slope (in the relation between ln*f* and ln PA signal). If f_c is the characteristic frequency of the sample of thickness, L, then α can be calculated from [12, 17]:

$$\alpha = f_c L^2 \tag{2}$$

The PA signal amplitude was recorded at various chopping frequencies (f) for each sample (depth profile analysis). The plots of ln(PA) amplitude vs. ln(*f*) are shown in Fig. 5a, b for representative SWCNTs/PMMA nanocomposite films of SWCNTs concentrations (0.5 and 2.0 wt%). The calculated values of α for these samples are given in Table 1. It is clearly seen that the measured value of α for the plain PMMA film without SWCNTs addition (pure) is 1.25×10^{-7} m²/s, which is very close to the reported value of α for PMMA (=1.11×10^{-7} m²/s) [22]. Moreover, there is 98 % enhancement of α from its original

Table 1 The values of thermal diffusivity (α), thermal effusivity (e) and thermal conductivity (k) for different concentrations of SWCNTs/PMMA

SWCNTs concentration (wt%)	Thermal diffusivity (α) (10^{-7} m²/s) ±0.1	Thermal effusivity (e) (Ws$^{1/2}$m^{-2}K^{-1}) ±7	Thermal conductivity (k) (W/m K) ±0.02
0	1.25	644	0.23
0.5	1.43	839	0.32
1.0	1.67	858	0.35
1.5	1.89	931	0.41
2.0	2.48	1,226	0.61
Pure SWCNTs	–	–	6,000 [28]

value by increases in SWCNTs ratio for 2.0 wt% SWCNTs concentration.

Thermal effusivity (e) is another thermal quantity that can be measured by PA technique, which is a measure of its ability to exchange thermal energy with its surroundings and gives information about the surface heating of the substances. As mentioned before, in case of thermally thick and optically opaque samples, the amplitude of the PA signal "q" is given by [23, 24];

$$q = \frac{B}{e}\frac{1}{f} \tag{3}$$

where $B = \frac{I_0}{2}\frac{\gamma P_0 \alpha_g}{2\pi l_g T_0}^{1/2}$, I_0 is the incident light intensity, γ is the ratio of specific heats, P_0 is the ambient pressure, α_g is the gas thermal diffusivity, l_g is the length of the gas column, T_0 is the ambient temperature, and f is the modulation frequency.

Using Si wafer as a reference sample, with a well-known thermal effusivity (16,060 Ws$^{1/2}$m^{-2}K^{-1} [24]). The constant factor, B, is calculated by normalizing the signal measured for the sample to that measured for Si. The obtained e values for samples with SWCNTs concentration from 0.5 to 2.0 wt% are also given in Table 1, where the slopes of Si and the samples were obtained from Fig. 6 by
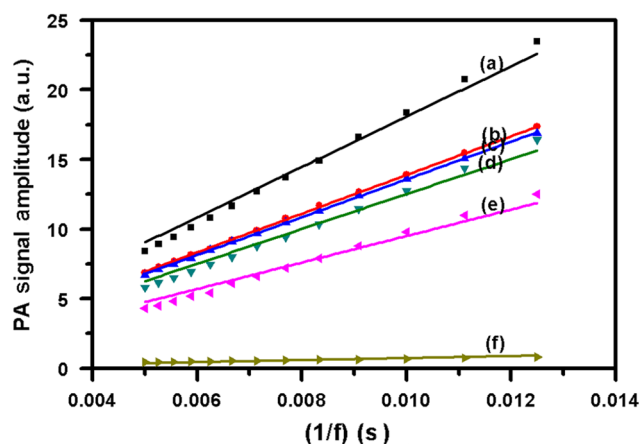
Fig. 6 PA signal amplitude vs. (1/f) for: **a** plain PMMA, **b** 0.5 wt%, **c** 1.0 wt%, **d** 1.5 wt%, **e** 2.0 wt% concentrations of SWCNTs/PMMA and **f** Si as a reference

Fig. 7 Thermal conductivity of SWCNTs/PMMA nanocomposite films as a function of SWCNTs concentration

linear fitting for the relation between (1/f) and PA amplitude (q). The results show that the values of e for SWCNTs/PMMA increases from 644 to 1,226 $Ws^{1/2}/m^2$ K as the concentration of SWCNTs increases from 0 to 2.0 wt%.

Finally, thermal conductivity (k) is one of the most important thermal parameters, which is considered as an indicator of the material. The measured values of α and e are used to calculate k for all films from the relation [9, 25, 26]:

$$k = e\sqrt{\alpha} \qquad (4)$$

The calculated values of k are also displayed in Table 1. It can be seen that the values of k for the plain PMMA is 0.23 W/m K, which is very close to the reported value of k for PMMA (0.21 W/m K) [27]. The measured values of k for our composite samples as a function of concentration of SWCNTs from 0 to 2.0 wt% are presented in Fig. 7. There is again an increase in k with increasing SWCNTs concentration. The increase in k is more significant ($\approx$160 %) at 2.0 wt% SWCNTs concentration. Mainly, this increase is due to the presence of a new phase (for SWCNTs) with high thermal conductivity, which increases the heat flow in the composite. This increase is noticeable and more significant as the concentration of CNTs increases. Such enhancement in k with increasing CNTs concentration was reported by other authors [1, 27, 28]. Mazov et al. [28] recorded the thermal conductivity of polypropylene-based composites with multiwall carbon nanotubes (MWCT) with different diameters, morphology and different MWCT concentrations (0–17 wt%). They concluded that there is a continuous increase of thermal conductivity value up to the highest concentrations (i.e., 16–17 wt%) thus reaching value of 0.55–0.56 W/m K. Moreover, fairly similar results were obtained by Han et al.
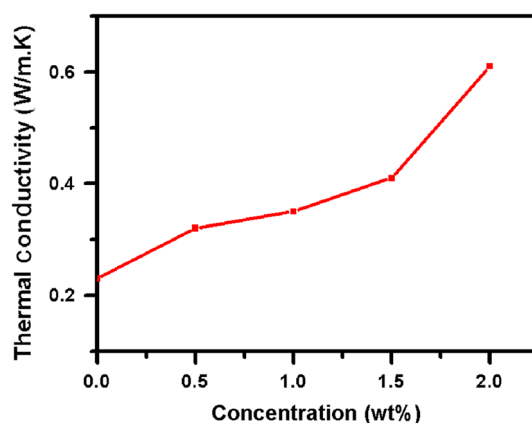
[27]. In their work, they concluded that many factors such as CNTs aspect ratio, mixing conditions, alignments and others affect the enhancement of thermal conductivity of CNTs composites.

The conduction of heat in polymer such as PMMA may be considered as the propagation of harmonic elastic waves through a continuum and propagation occurs via interaction of the quanta of thermal energy called "phonons". In this case, the thermal conductivity, k, is given by [27]:

$$k = \frac{C_p vl}{3} \qquad (5)$$

where C_p is the specific heat capacity per unit volume, v is the average phonon velocity, and l is the phonon mean free path. For PMMA, l is extremely small due to phonon scattering from numerous defects leading to reduce l and in turn k. However, the very weak dependence on filler content for C_p and v leads to the fact that the mean free path of thermal energy carrier essentially determines the thermal diffusivity value and consequently thermal conductivity. For an SWCNTs/PMMA nanocomposite, the thermal parameters (α and k) depend upon the connectivity area of contact between the SWCNTs and its thermal conductivity. In the present case, the increase in SWCNTs concentration leads to higher connectivity, which leads to fewer scattering center and consequent increase in the mean free path of thermal energy carrier (phonon). This argument explains the observed increase in α and k. Besides that the presence of a new phase with high thermal conductivity leads to increase in the heat flow [1].

Electrical properties measurements

Figure 8 shows the DC electrical conductivity (σ) of the SWCNTs/PMMA composite films from 0 to 10.0 wt% SWCNTs concentrations at room temperature. The results
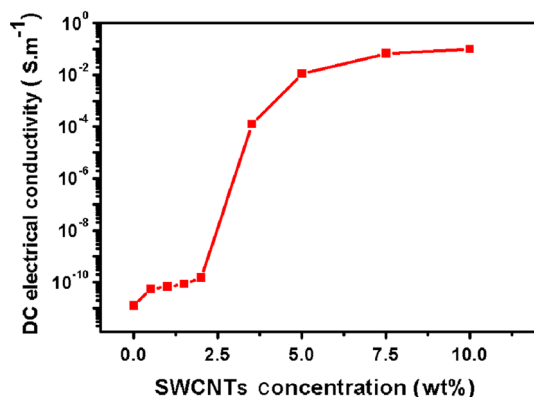
Springer

Fig. 8 DC electrical conductivity for SWCNTs/PMMA nanocomposite films of different concentrations

show that the value of σ for plain PMMA film was about 1.3×10^{-11} S m^{-1}. It is clearly seen that σ increases about four orders of magnitude as SWCNTs concentration increases from 2.0 to 3.5 wt%. The percolation threshold value is about 2.0 wt% of SWCNTs loading. Our result is in good agreement with previous studies for SWCNT/polymer composites [29]. We believe that the increase in σ may be due to the creation of extensive conductive networks due to the high electrical conductivity of the filler (SWCNTs) that facilitate electrons transport in the composite when SWCNTs concentrations increase. In other words, as the SWCNTs approach each other by increasing SWCNTs concentration, the current can flow even through without direct contacts between SWCNTs. This mechanism is well known and called "quantum mechanical tunneling" [1], where electrons can move through the insulator between conductive elements (CNT) with a certain probability. Our results are in good agreement with others [8, 30, 31]. Chu et al. [30] concluded that the DC electrical conductivity is enhanced as the CNT loading increases reaching the percolation threshold where the conductive path of the interconnected CNTs is formed across the volume of the composite.

Conclusion

Composite films of SWCNTs/PMMA have been fabricated with SWCNTs loading up to 10.0 wt% using casting technique. The absorption intensity of the composite was enhanced ≈ 8.5 times compared to the plain PMMA. Furthermore, the thermophysical parameters including α, e and k were obtained using PA technique. We demonstrated a 160 % increase in k with SWCNTs loading of 2.0 wt%. The increase in k with the increasing in CNTs loading was attributed to the enhancement of connectivity

which resulted in a decrease in scattering center and consequent increase in the mean free path of the thermal energy carrier (phonon). The DC electrical conductivity measurements of SWCNTs/PMMA films showed that the percolation threshold value was about 2.0 wt%.

References

1. Aljaafari AA, Ibrahim SS, El-Brolossy TA (2011) Thermophysical and electrical characterization of PVC–SWNT nanocomposites. Compos Part A: Appl Sci Manufact 42:394–399
2. Pradhan A, Swain S (2013) Synthesis and characterization of poly(acrylonitrile-co-methylmethacrylate) nanocomposites reinforced by functionalized multiwalled carbon nanotubes. Iran Polym J 22:369–376
3. Alimardani M, Abbassi-Sourki F, Bakhshandeh G (2012) Preparation and characterization of carboxylated styrene butadiene rubber (XSBR)/multiwall carbon nanotubes (MWCNTs) nanocomposites. Iran Polym J 21:809–820
4. Hajibaba A, Naderi G, Ghoreishy M, Bakhshandeh G, Nouri M (2012) Effect of single-walled carbon nanotubes on morphology and mechanical properties of NBR/PVC blends. Iran Polym J 21:505–511
5. Zamani M, Fereidoon A, Sabet A (2012) Multi-walled carbon nanotube-filled polypropylene nanocomposites: high velocity impact response and mechanical properties. Iran Polym J 21:887–894
6. Aarab H, Bätoul M, W'ery J, Almairac R, Lefrant S, Faulques E, Duvail JL, Hamedoun M (2005) Electrical and optical properties of PPV and single-walled carbon nanotubes composite films. Synth Met 155:63–67
7. Bal S, Samal SS (2007) Carbon nanotube reinforced polymer composites—a state of the art. Bull Mater Sci 30:379–386
8. Peng H, Sun X (2009) Highly aligned carbon nanotube/polymer composites with much improved electrical conductivities. Chem Phys Lett 471:103–105
9. Badawi A, Al-Hosiny N, Abdallah S, Negm S, Talaat H (2012) Photoacoustic study of optical and thermal properties of CdTe quantum dots. J Mater Sci Eng A 2:1–6
10. Rosencwaig A, Gersho A (1976) Theory of the photoacoustic effect with solids. J Appl Phys 47:65–69
11. Yu J, Fan J, Cheng B (2011) Dye-sensitized solar cells based on anatase TiO$_2$ hollow spheres/carbon nanotube composite films. J Power Sources 196:7891–7898
12. Al-Hosiny NM, Abdallah S, Moussa MAA, Badawi A (2013) Optical, thermophysical and electrical characterization of PMMA (CdSe QDs) composite films. J Polym Res 20:1–8
13. Tomar AK, Mahendia S, Kumar S (2011) Structural characterization of PMMA blended with chemically synthesized PAni. Adv Appl Sci Res 2:327–333
14. Lafuente E, Callejas MA, Sainz R, Benito AM, Maser WK, Sanjuan ML, Saurel D, Teresa JM, Martinez MT (2008) The influence of single-walled carbon nanotube functionalization on the electronic properties of their polyaniline composites. 46:1909–1917
15. Oh W-C, Chen M-L (2008) Synthesis and characterization of CNT/TiO$_2$ composites thermally derived from MWCNT and titanium(IV) n-butoxide. Bull Korean Chem Soc 29:159–164

16. Devi JM, Ali KS, Venkatraman VR, Ramakrishnan SK, Ramachandran K (2005) A study on the thermal properties of cinnamoyl chalcones. Thermochim Acta 438:29–34

17. Raji P, Ramachandran K, Sanjeeviraja C (2006) Thermal and optical properties of $Cd_{1-x}Zn_xS$ thin films by photoacoustics. J Mater Sci 41:5907–5914

18. Raji P, Sanjeeviraja C, Ramachandran K (2004) Thermal properties of nano crystalline CdS. Cryst Res Technol 39:617–622

19. Raji P, Sanjeeviraja C, Ramachandran K (2005) Thermal and structural properties of spray pyrolysed CdS thin film. Bull Mater Sci 28:233–238

20. El-Brolossy TA, Abdallah S, Abdallah T, Mohamed MB, Negm S, Talaat H (2008) Photoacoustic characterization of optical and thermal properties of CdSe quantum dots. Eur Phys J Special Topics 153:365–368

21. Toyoda T, Hayakawa T, Shen Q (2000) Photoacoustic, photoelectrochemical current, and photoluminescence spectra of highly porous, polycrystalline TiO_2 electrodes fabricated by chemical synthesis. Mater Sci and Eng B 78:84–89

22. Friederich B, Laachachi A, Ferriol M, Ruch D, Cochez M, Toniazzo V (2010) Tentative links between thermal diffusivity and fire-retardant properties in poly(methyl methacrylate)–metal oxide nanocomposites. Polym Degrad Stabil 95:1183–1193

23. Poulet P, Chambron J, Unterreiner R (1980) Quantitative photoacoustic spectroscopy applied to thermally thick samples. J Appl Phys 51:1738–1742

24. Al-Hosiny N, Badawi A, Moussa MAA, El-Agmy R, Abdallah S (2012) Characterization of optical and thermal properties of CdSe quantum dots using photoacoustic technique. Int J Nanopart 5:258–266

25. Abdallah S, Easawi K, Negm S, Youssef GM, El-Brolossy TA, Talaat H (2003) Determination of thermophysical parameters of porous silicon using a photothermal technique. Rev Sci Instrum 74:848–850

26. Srinivasan R, Ramachandran K (2008) Synthesis and thermal diffusion of nanostructured porous GaAs. Cryst Res Technol 43:953–958

27. Han Z, Fina A (2011) Thermal conductivity of carbon nanotubes and their polymer nanocomposites: a review. Prog Polym Sci 36:914–944

28. Mazov IN, Ilinykh IA, Kuznetsov VL, Stepashkin AA, Ergin KS, Muratov DS, Tcherdyntsev VV, Kuznetsov DV, Issi JP (2014) Thermal conductivity of polypropylene-based composites with multiwall carbon nanotubes with different diameter and morphology. J Alloy Compound 586:S440–S442

29. Huang Y, Li N, Ma Y, Du F, Li F, He X, Lin X, Gao H, Chen Y (2007) The influence of single-walled carbon nanotube structure on the electromagnetic interference shielding efficiency of its epoxy composites. Carbon 45:1614–1621

30. Chu C–C, White KL, Liu P, Zhang X, Sue H-J (2012) Electrical conductivity and thermal stability of polypropylene containing well-dispersed multi-walled carbon nanotubes disentangled with exfoliated nanoplatelets. Carbon 50:4711–4721

31. Ma P-C, Siddiqui NA, Marom G, Kim J-K (2010) Dispersion and functionalization of carbon nanotubes for polymer-based nanocomposites: a review. Compos A 41:1345–1367